ORIGINAL PAPER

Computational structural analysis of composites with spectral-based stochastic multi-scale method

Jie Zhi[1] · Tong-Earn Tay[1]

Abstract

Composite materials and structures may be characterized at different length scales, ranging from the micro-scale at the fiber–matrix level, meso-scale at the lamina–laminate level, to structural macro-scale. However, uncertainties in material properties and geometric parameters due to manufacturing, defects and assembly processes may occur at various length scales. This paper presents a computational framework for stochastic analysis of composites with consideration of stochastic parameters at micro- and meso-scales. The novelty of the proposed framework is the integration of the spectral stochastic finite element method and asymptotic homogenization method within a finite element technique, which was implemented through ABAQUS®. This spectral stochastic homogenization method efficiently predicts the propagation of uncertainties from the constituent to ply levels. The derived probability distributions of effective properties were verified by Monte Carlo simulation. Another novelty is the study of the influence of stochastic parameters at both micro-scale and meso-scale on the failure prediction of composite structures, without assumptions of probabilistic characteristic of ply properties commonly used in a single-scale stochastic analysis. The up-scaled uncertainties combined with other randomness at meso-scale (strength properties and ply orientations) are provided as the input of meso-scale stochastic strength analysis of a quasi-isotropic laminate based on classical lamination theory (CLT) and ply discount. The probability distribution of first-ply failure and ultimate failure loads are obtained and their sensitivity factors with respect to input variations are presented.

Keywords Stochastic homogenization · Probabilistic strength · Polynomial chaos · Spectral stochastic method · Monte Carlo simulation

1 Introduction

Fiber-reinforced polymer–matrix composites have been widely applied in many industries (e.g., aerospace engineering) due to their excellent properties and tailored-design capability. Recently, there have been efforts to develop multi-scale simulation strategies across different length scales (constituent, ply and laminate level, usually denoted by micro-, meso- and macro-scale, respectively) (Lorca et al. 2011). However, statistical uncertainties in properties at micro- and meso-scales (Chamis 2004) can arise due to various sources such as manufacturing defects, variable constituent properties, damage, voids, etc., as shown in Fig. 1. Deterministic
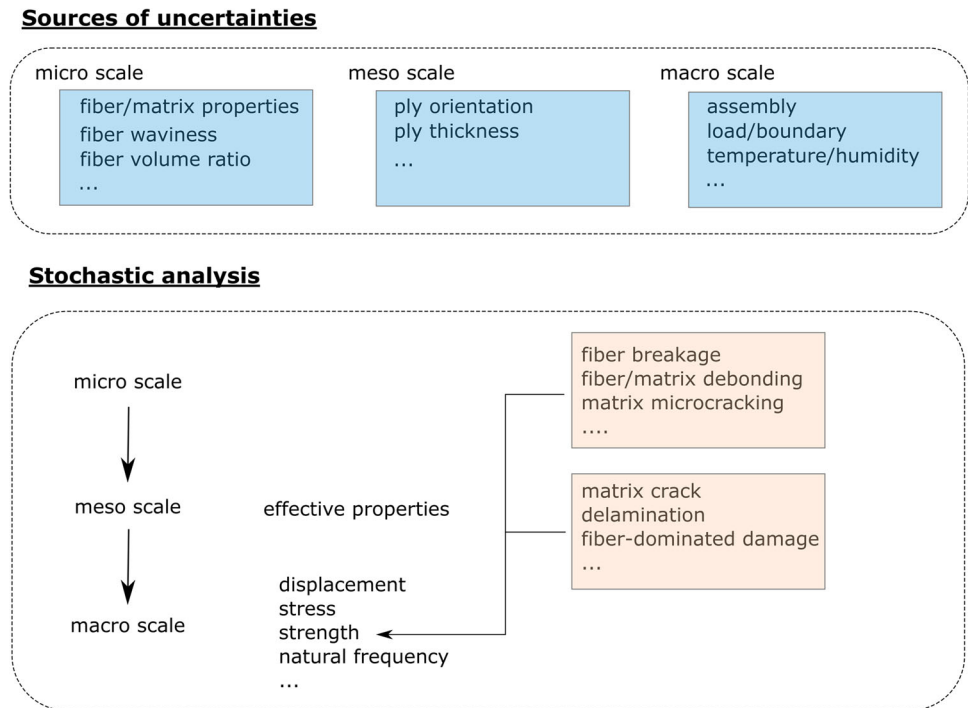
approaches implicitly account for uncertainties in predictive models through safety factors, which may be excessively conservative. Therefore, some recent efforts to incorporate uncertainties quantitatively in design and analysis of composites have been proposed in the literature (Sriramula and Chryssanthopoulos 2009; Chiachio et al. 2012; Dey et al. 2017).

As shown in Fig. 1, typical stochastic responses of composite structures at macro-scale include displacement, stress, strength and natural frequency, which can be obtained based on ply properties directly or effective properties derived from micro- scales (Sriramula and Chryssanthopoulos 2009). Strength analysis is of special interest due to the requirement of structural integrity and the complicated damage patterns of composites at both micro- and meso-scales, as indicated in Fig. 1. The study of failure mechanism in composites could be enhanced with consideration of stochastic factors, such as stochastic material properties (e.g., strength) and geometric randomness (e.g., fiber distribution) in the simulation

✉ Jie Zhi
jie.zhi@u.nus.edu

[1] Department of Mechanical Engineering, National University of Singapore, 21 Lower Kent Ridge Road, Singapore 119077, Singapore

Fig. 1 Sources of uncertainties
and stochastic analysis of failure
of composites

Sources of uncertainties

micro scale

fiber/matrix properties
fiber waviness
fiber volume ratio
...

meso scale

ply orientation
ply thickness
...

macro scale

assembly
load/boundary
temperature/humidity
...

Stochastic analysis

micro scale

meso scale   effective properties

macro scale

fiber breakage
fiber/matrix debonding
matrix microcracking
....

matrix crack
delamination
fiber-dominated damage
...

displacement
stress
strength
natural frequency
...

of intralaminar damage, including fiber breakage (Swolfs et al. 2016; St-Pierre et al. 2017; Pimenta and Pinho 2013; Pimenta 2017) and transverse matrix cracking (Vinogradov and Hashin 2005; Andersons et al. 2008). Although it is ideal to consider each failure patterns faithfully to achieve high-fidelity simulations, nonlinear computational models involving damage processes are too computationally intensive in design applications, where multiple design variables are involved. When reliability or risk of failure of composite structures (Chiachio et al. 2012) is required to be assessed, efficiency becomes particularly important and simple analytical models or linear finite element analysis are preferred.

Furthermore, stochastic finite element methods (SFEM) have been employed to solve static and dynamic problems (Stefanou 2009; Arregui-Mena et al. 2016). The Monte Carlo simulation (MCS) is a general and direct approach for generating parametric and geometric randomness. Since the solution of large number of MC simulations via sample problems is not computationally viable, various metamodel or surrogate models, such as response surface methodology, artificial neural network and kriging (Dey et al. 2017), are alternative approaches. If only parametric uncertainties are considered, the perturbation method and the spectral stochastic method (Stefanou 2009) may be employed. The perturbation method characterizes the random feature by the Taylor series expansion of stochastic FE matrix and response vectors. It is relatively efficient compared to MCS and useful in estimating the statistical moments of stochastic response. However, the nature of Taylor series expansion means it is only applicable to problems with small random variations.

The spectral stochastic method introduced by Ghanem and Spanos (2003) involves not only the discretization with FE in spatial dimension but also the approximation with polynomial chaos (PC) expansion in stochastic space, the error of which is minimized through the Galerkin approach. The advantages of this method are that only one deterministic equation needs to be solved and the whole probabilistic structure of quantities of interest can then be obtained.

Early work on computational stochastic analysis of composite structures was mostly conducted at ply level. Vinckenroy and Wilde (1995) adopted MCS combined with FE modeling and evaluated the variation of maximum stress in an open-hole composite plate due to randomness in material properties (E_1, E_2, v_{12}) and geometric parameters (hole size and position). Probabilistic strength analysis was developed by Jeong and Shenoi (2000) based on MCS and first-ply failure analysis with applied load, elastic moduli, geometric and strength values assumed as random variables following normal and Weibull probability distributions. Spatial variation of strength properties was considered by Wu et al. (2000) who used a random field model with MCS and FPF based on Tsai–Hill and Tsai–Wu criteria. The importance of including the variability of material elastic properties in reliability analysis of laminates was demonstrated by Lekou and Philippidis (2008) and an overestimation of reliability could be caused without considering these variabilities. Sánchez-Heres et al. (2014) further investigated the influence of mechanical models for laminate failure and probabilistic models for ply properties on reliability estimation of cross-ply laminates. Among all the factors, the definition and modeling of matrix

cracking in mechanical models (failure criteria and ply discounts) and the choice of probability distribution (normal, Weibull and log-normal distributions) have comparatively large influence. Other applications in composites with MCS or related metamodels include strength analysis with spatial variation of loading position (Karsh et al. 2018), buckling analysis (Kepple et al. 2015), free vibration analysis (Dey et al. 2015; Chakraborty et al. 2016) and strength analysis of joints (Vijaya Kumar and Bhat 2015; Zhao et al. 2017).

First-order perturbation technique was adopted by Onkar et al. (2007) to improve the efficacy in predicting the statistics of the first-ply failure load of composite plates with random material properties subject to uniform distributed random load. Lal et al. (2009, 2011) studied the effect of random system properties such as material properties and laminate thickness on thermal buckling load and post buckling load of composite plates using higher order shear deformation plate theory and first-order perturbation technique. While stiffnesses are usually taken as random variables, Noh and Park (2011) focused on the spatial randomness of Poisson's ratio and statistical moments of displacement were calculated with first-order Taylor-series expansion. However, the computed variation in response is not significant (coefficient of variation is 1.0–6.0%, the input variation is 0.1), which suggests the variation in Poisson's ratio may not be critical. The correlation among random variables for composite structures (e.g., E_{11} and E_{22}) was considered in a recent work based on the combination of the Perturbation method and so-called Copula function (a tie function linking the marginal cumulative distribution with joint cumulative distribution), which mitigates the defects of traditional transformation method in terms of efficiency, accuracy and application (Cui et al. 2017). The spectral stochastic method has also attracted many applications in modeling composite structures. Chung et al. (2005) implemented a spectral stochastic version of solid-like shell element within an object-oriented computational framework and applied it to fiber metal laminates with the material properties of glass fiber epoxy layers treated as independent random field models. Ngah and Young (2007) compared the accuracy of the perturbation method and the spectral stochastic method in the stochastic analysis of a rectangular unidirectional composite panel with structural stiffness assumed as a Gaussian random field. It shows that the former method is only efficient for low material variability (coefficient of variation up to 10%) while the later method can achieve accurate results with a comparatively large material variability (24%). Chen and Soares (2008) extended the application of spectral method to multi-layer laminates and various moduli (E_1, G_{12}, G_{23}, G_{13}) were modeled as independent random fields. The accuracy and efficiency of this developed formulation were benchmarked through MCS. Other recent applications include free vibration analysis (Sepahvand 2016), aeroelastic response analysis

(Scarth et al. 2014) and stochastic analysis of composite structures with both normal random and interval variables (Chen and Qiu 2018).

In meso-scale stochastic analysis, assumptions regarding the probabilistic characteristics of material properties are often difficult to justify (Charmpis et al. 2007). Charmpis et al. (2007) proposes that macro-properties be derived from micro-mechanical stochastic information. Therefore, only the stochastic constituent properties need to be quantified. By casting simple analytical micro-mechanical model in a probabilistic framework, Shaw et al. (2010) derived macro-level statistics for reliability analysis of composites with MCS. Stochastic fiber and matrix properties as well as volume fraction were also considered by Li et al. (2016) in the stochastic thermal buckling analysis of laminated plates using perturbation method. Other analytical homogenization methods include self-consistent model and differential model explored by Ma et al. (2011). Although stochastic analytical homogenization method is simple and fast due to the closed formulations, the simplified assumptions limit their applications. Hence, stochastic computational homogenization has received more attention recently. Perturbation-based stochastic finite element method was first developed by Kamiński and Kleiber (2000). Sakata et al. (2008) extended the perturbation-based stochastic homogenization to detailed three-dimensional analysis and considered randomness in Young's modulus and Poisson's ratio of constituent materials. They conclude that the perturbation-based method does not perform well for nonlinear stochastic problems with large variations. A recently developed computational homogenization method Perić et al. (2011) was implemented with a second-order perturbation technique by Zhou et al. (2016a, b) for the stochastic homogenization of unidirectional composites and woven textile composites. The multi-scale uncertainty issue was later addressed in reliability analyses for composite structures (Zhou et al. 2016c, 2017). However, besides being inaccurate in applications with large variation, the perturbation-based analysis is unable to predict probability distribution. The spectral stochastic method is promising in solving this problem but related research work still remains few (Tootkaboni and Graham-Brady 2010). Other recent work includes the application of artificial neural networks (Balokas et al. 2017) and interval method (Chen et al. 2017).

The above review has shown that although numerous work has been conducted for stochastic analysis of composites based on randomness at meso-scale with various methods, there has been more recent work exploring randomness at the micro-scale level. However, work on uncertainty propagation from micro-properties to macro-response still remains few, with the exception of recent work by Zhou et al. (2016c, 2017) based on the perturbation method. Considering the aforementioned advantages of the spectral

stochastic method, we propose a computational framework for spectral stochastic multi-scale analysis of composites structures. The structure of this paper is organized as follows. In Sect. 2, the formulation of spectral-based stochastic multi-scale methods is presented for both homogenization and macro-analysis. The numerical implementation is detailed in Sect. 3. Section 4 shows the predicted stochastic outputs including stochastic effective properties and stochastic macro-behavior. Conclusions are drawn in Sect. 5.

2 Spectral-based stochastic multi-scale methods

In this section, we present the stochastic formulation of a hierarchical multi-scale analysis of fiber-reinforced composites, where a computational homogenization is adopted to obtain the effective properties prior to the macro-analysis. The spectral stochastic method is introduced to solve this uncertainty propagation problem. The subsequent macro-failure analysis is then conducted based on the stochastic effective properties and other uncertainties obtained at meso-scale.

2.1 Stochastic formulation of asymptotic homogenization

In computational homogenization methods, a representative volume element (RVE) is usually adopted to calculate effective properties based on asymptotic method (Kamiński and Kleiber 2000) and Hill–Mandel macro-homogeneity condition (Zhou et al. 2016a). As shown in Fig. 2, besides the original scale x, another length scale $y = x/\zeta$ ($\zeta \ll 1$) is introduced to describe the fast variable, corresponding to macro-scale and micro-scale in the context of composites, respectively. Assuming periodic micro-structure, the stiffness tensor is a function of properties at the micro-scale

$$\mathbb{D}^{\zeta}(x) = \mathbb{D}(y) = \mathbb{D}(x/\zeta), \tag{1}$$

where superscript ζ denotes the ζ Y-periodicity in the system of coordinates x. Considering randomness in the stiffness
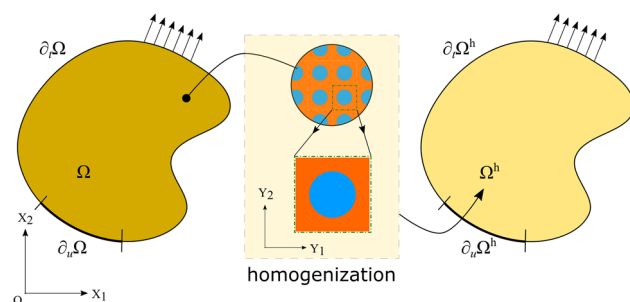

Fig. 2 Illustration of homogenization method

tensor, the strong form of original boundary value problem can be written as:

$$\begin{aligned}
&\nabla^{\zeta} \cdot \sigma^{\zeta}(x, \xi) + b = 0, \quad \text{in } \Omega; \\
&\sigma^{\zeta}(x, \xi) = \mathbb{D}^{\zeta}(x, \xi) : \epsilon^{\zeta}(x, \xi), \quad \text{in } \Omega; \\
&\epsilon^{\zeta}(x, \xi) = ((\nabla^{\zeta} u^{\zeta}(x, \xi))^T + \nabla^{\zeta} u^{\zeta}(x, \xi))/2, \quad \text{in } \Omega; \\
&u^{\zeta} = \hat{u} \quad \text{on } \partial_u \Omega; \quad \sigma^{\zeta} \cdot n = \hat{t} \quad \text{on } \partial_t \Omega;
\end{aligned} \tag{2}$$

where ξ is a vector of random variables and $\nabla^{\zeta} = \nabla_x + \nabla_y/\zeta$ according to the chain rule.

A double-scale asymptotic expansion of displacement field is expressed as:

$$\begin{aligned}
u^{\zeta}(x, \xi) = u^{(0)}(x, y, \xi) + \zeta u^{(1)}(x, y, \xi) \\
+ \zeta^2 u^{(2)}(x, y, \xi) + O(\zeta^3),
\end{aligned} \tag{3}$$

where $u^{(0)}(x, y, \xi) = u^{(0)}(x, \xi)$. Then strain and stress can be derived as:

$$\begin{aligned}
\epsilon^{\zeta}(x, \xi) &= \zeta^{-1} \epsilon^{(0)}(x, y, \xi) + \epsilon^{(1)}(x, y, \xi) \\
&\quad + \zeta^1 \epsilon^{(2)}(x, y, \xi) + O(\zeta^2), \\
\sigma^{\zeta}(x, \xi) &= \zeta^{-1} \sigma^{(0)}(x, y, \xi) + \sigma^{(1)}(x, y, \xi) \\
&\quad + \zeta^1 \sigma^{(2)}(x, y, \xi) + O(\zeta^2).
\end{aligned} \tag{4}$$

With these expansions, the two-scale problem can be derived directly by substituting Eqs. (3) and (4) into Eq. (2) or through a variational form. The homogenized problem can then be given by:

$$\begin{aligned}
&\nabla_x \cdot \sigma^h(x, \xi) + b = 0, \quad \text{in } \Omega^h; \\
&\sigma^h(x, \xi) = \mathbb{D}^h(x, \xi) : \epsilon^h(x, \xi), \quad \text{in } \Omega^h; \\
&\epsilon^h(x, \xi) = ((\nabla_x u^h(x, \xi))^T + \nabla_x u^h(x, \xi))/2, \quad \text{in } \Omega^h; \\
&u^h = \hat{u} \quad \text{on } \partial_u \Omega^h; \quad \sigma^h \cdot n = \hat{t} \quad \text{on } \partial_t \Omega^h;
\end{aligned} \tag{5}$$

where superscript h denotes homogenization.

Effective properties of composites can be derived from the homogenized stiffness tensor $\mathbb{D}^h(\cdot, \xi)$, which is given by:

$$\mathbb{D}^h(\cdot, \xi) = \frac{1}{|Y|} \int_Y \mathbb{D}(y, \xi) : (\mathbb{I} - \nabla_y \chi(y, \xi))^T \, dy, \tag{6}$$

where $\chi(y, \xi)$ is the characteristic displacement tensor of third-order which is determined by:

$$\nabla_y \cdot (\mathbb{D}(y, \xi) : (\mathbb{I} - \nabla_y \chi(y, \xi))^T) = 0. \tag{7}$$

For the purpose of numerical solution, weak formulations can be written as:

$$\int_Y \nabla_y \boldsymbol{v} : \mathbb{D}(\boldsymbol{y}, \boldsymbol{\xi}) : (\nabla_y \boldsymbol{\chi}(\boldsymbol{y}, \boldsymbol{\xi}))^T \mathrm{d}y$$
$$= \int_Y \nabla_y \boldsymbol{v} : \mathbb{D}(\boldsymbol{y}, \boldsymbol{\xi}) \mathrm{d}y, \quad \forall \boldsymbol{v} \in \tilde{V}_Y, \tag{8}$$

where $\tilde{V}_Y$ is the set of Y-periodic continuous and sufficiently regular functions with zero average in Y. Equation (8) is usually solved by FEM, the matrix form of which is given by:

$$\mathop{\mathbf{A}}_{e=1}^{n_{ele}} \left(\int_{Y^e} \boldsymbol{B}^{eT} \boldsymbol{D}^e(\boldsymbol{\xi}) \boldsymbol{B}^e \mathrm{d}y \boldsymbol{\chi}^e(\boldsymbol{\xi}) \right) = \mathop{\mathbf{A}}_{e=1}^{n_{ele}} \left(\int_{Y^e} \boldsymbol{B}^{eT} \boldsymbol{D}^e(\boldsymbol{\xi}) \mathrm{d}y \right), \tag{9}$$

where n_{ele} is the number of elements used for discretizing the RVE and $\boldsymbol{B}^e$ is strain displacement matrix.

The solution of Eq. (9) is then substituted into Eq. (6) and the homogenized stiffness matrix can be obtained as:

$$\boldsymbol{D}^h(\boldsymbol{\xi}) = \sum_{e=1}^{n_{ele}} \frac{V_e}{V_{tot}} \boldsymbol{D}^e(\boldsymbol{\xi})(\boldsymbol{I} - \boldsymbol{B}^e \boldsymbol{\chi}^e(\boldsymbol{\xi})), \tag{10}$$

where V_{tot} is the volume of RVE and V_e is the volume of a single element. As seen from Eqs. (9) and (10), the randomness of homogenized stiffness matrix originates in the properties of fiber and matrix $\boldsymbol{D}^e(\boldsymbol{\xi})$. The probability distribution of effective properties $\boldsymbol{D}^h(\boldsymbol{\xi})$, may be directly obtained by repeatedly generating samples of $\boldsymbol{D}^e(\boldsymbol{\xi})$ and solving Eqs. (9) and (10) but it is inefficient and very time-consuming. Thus, a non-sampling method is introduced in the following section.

2.2 Spectral stochastic homogenization method

The spectral stochastic method adopts polynomial chaos (PC) expansions to discretize random variables in stochastic space. It is sometimes used with finite element method and thus also termed spectral stochastic finite element method. This method is initially developed to solve stochastic linear static problems but is employed here for stochastic homogenization. Suppose the input stochastic parameters can be expressed as a linear combination of random variables

$$\boldsymbol{D}^e(\boldsymbol{\xi}) = \sum_{i=0}^{N-1} \boldsymbol{D}_i^e \xi_i \tag{11}$$

and approximation of solution variables in Eq. (9) can be expressed with polynomial chaos (orthogonal polynomials in terms of random variables)

$$\boldsymbol{\chi}^e(\boldsymbol{\xi}) = \boldsymbol{\chi}_0^e \Gamma_0 + \sum_{i=1}^N \boldsymbol{\chi}_i^e \Gamma_1(\xi_i) + \sum_{i=1}^N \sum_{j=1}^i \boldsymbol{\chi}_{ij}^e \Gamma_2(\xi_i, \xi_j) + \cdots, \tag{12}$$

where Γ_p denotes the polynomial chaos of order p. Equation (12) may be truncated after the pth order polynomial chaos terms and expressed in a compact form

$$\boldsymbol{\chi}^e(\boldsymbol{\xi}) \approx \sum_{j=0}^{P_\chi - 1} \boldsymbol{X}_j^e \Psi_j(\boldsymbol{\xi}), \tag{13}$$

where the stochastic basis $\Psi_j(\boldsymbol{\xi})$ satisfies

$$\Psi_0(\boldsymbol{\xi}) \equiv 1, \; E[\Psi_j(\boldsymbol{\xi})] = 0, \; E[\Psi_j(\boldsymbol{\xi})\Psi_k(\boldsymbol{\xi})] = 0 \, (j > 0, \, j \neq k), \tag{14}$$

where $E[\cdot]$ denotes expectation operator and the remaining polynomial chaos terms are given by:

$$P_\chi = \frac{(N+p)!}{N!p!}. \tag{15}$$

The Hermite polynomial chaos expansion was used by (Ghanem and Spanos 2003) for problems with Gaussian random variables and generalized polynomial chaos expansion for various types of random variables (Xiu 2010).

Substituting Eqs. (11) and (13) into Eq. (9), the approximation error can be minimized through Galerkin approach

$$\mathop{\mathbf{A}}_{e=1}^{n_{ele}} (\boldsymbol{k}^e \boldsymbol{X}^e) = \mathop{\mathbf{A}}_{e=1}^{n_{ele}} (\boldsymbol{f}^e);$$
$$\boldsymbol{k}_{jk}^e = \sum_{i=0}^{N-1} \int_{Y^e} \boldsymbol{B}^{eT} \boldsymbol{D}_i^e \boldsymbol{B}^e \mathrm{d}y c_{ijk}, \; c_{ijk} = E[\xi_i \Psi_j(\boldsymbol{\xi}) \cdot \Psi_k(\boldsymbol{\xi})];$$
$$\boldsymbol{f}_k^e = \sum_{i=0}^{N-1} \int_{Y^e} \boldsymbol{B}^{eT} \boldsymbol{D}_i^e \mathrm{d}y d_{ik}, \; d_{ik} = E[\xi_i \cdot \Psi_k(\boldsymbol{\xi})];$$
$$j, k = 0, 1, \cdots, P_\chi - 1. \tag{16}$$

Since Eq. (16) is a set of deterministic linear equations, it can be readily solved with FE. The solution $\boldsymbol{X}^e$ is then substituted into Eq. (13) and explicit expressions of $\boldsymbol{\chi}^e(\boldsymbol{\xi})$ in terms of simple random variables (e.g., normal random variable) can be obtained. However, the stochastic homogenized stiffness matrix still cannot be derived directly through Eq. (10), which contains two parts of randomness $\boldsymbol{D}^e(\boldsymbol{\xi})$ and $\boldsymbol{\chi}^e(\boldsymbol{\xi})$.

Employing PC expansions again to the left hand side of Eq. (10)

$$\boldsymbol{D}^h(\boldsymbol{\xi}) = \sum_{m=0}^{Q_\chi - 1} \boldsymbol{D}_m^h \Psi_m(\boldsymbol{\xi}). \tag{17}$$
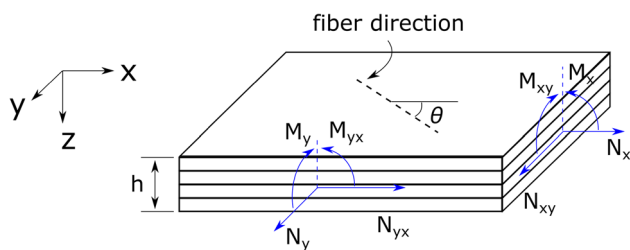
Fig. 3 Illustration of force and moment resultants on a composite laminate

For the sake of simplicity, $P_\chi = Q_\chi$ is assumed. Substituting Eqs. (11), (13) and (17) into Eq. (10), the coefficients of Eq. (17) can be obtained similarly as those of Eq. (13)

$$\bar{c}_{mm} D_m^h = \sum_{e=1}^{n_{ele}} \frac{V_e}{V_{tot}} \left(\sum_{i=0}^{N-1} D_i^e d_{im} - \sum_{i=0}^{N-1} \sum_{j=0}^{P_\chi-1} D_i^e B^e X_j^e c_{ijm} \right),$$

$$\bar{c}_{mm} = E[\Psi_m(\boldsymbol{\xi}) \cdot \Psi_m(\boldsymbol{\xi})]. \tag{18}$$

With the explicit expressions given by Eq. (17), the probability distribution of stochastic homogenized matrices can be obtained through sampling $\boldsymbol{\xi}$. The effective properties can be derived from compliance matrix $\boldsymbol{S}^h(\boldsymbol{\xi}) = (\boldsymbol{D}^h(\boldsymbol{\xi}))^{-1}$ given by:

$$\boldsymbol{S}^h(\boldsymbol{\xi}) = \begin{bmatrix} \frac{1}{E_1} & -\frac{v_{21}}{E_2} & -\frac{v_{31}}{E_3} & 0 & 0 & 0 \\ -\frac{v_{12}}{E_1} & \frac{1}{E_2} & -\frac{v_{32}}{E_3} & 0 & 0 & 0 \\ -\frac{v_{13}}{E_1} & -\frac{v_{23}}{E_2} & \frac{1}{E_3} & 0 & 0 & 0 \\ 0 & 0 & 0 & \frac{1}{G_{12}} & 0 & 0 \\ 0 & 0 & 0 & 0 & \frac{1}{G_{23}} & 0 \\ 0 & 0 & 0 & 0 & 0 & \frac{1}{G_{13}} \end{bmatrix}. \tag{19}$$

2.3 Stochastic failure analysis of laminates

Failure analysis of multi-layer laminates are critical to the design of composite structures. With complicated failure mechanisms presented in composites, various methods have been developed based on advanced finite elements (Tay et al. 2008). In design, classical lamination theory combined with a suitable failure criterion are used for reliability analysis of laminate plates (Nakayasu and Maekawa 1997; Lopez et al. 2014). Consider a laminate plate with n layers of fiber orientation $\theta_i(\boldsymbol{\eta})$, $i = 1, 2, \ldots, n$, where $\boldsymbol{\eta}$ denotes the randomness due to fiber misalignment at ply level. In Fig. 3, $N = \{N_x, N_y, N_{xy}\}$, $M = \{M_x, M_y, M_{xy}\}$ are resultant forces and moments per unit length applied along the edge. Based on Kirchhoff's hypothesis, the displacements can be parametrized by a translation and a rotation. The laminate strain in the global coordinate x–y–z is expressed as

$\boldsymbol{\epsilon} = \boldsymbol{\epsilon}^0 + z\boldsymbol{\kappa}$, where $\boldsymbol{\epsilon}^0$ and $\boldsymbol{\kappa}$ are midplane strains and curvatures (Kaw 2005). For the ith layer, the strain in the local material coordinate 1–2–z is $\boldsymbol{\epsilon}_{loc} = \boldsymbol{T}_1(\boldsymbol{\eta})\boldsymbol{\epsilon}$,

$$\begin{bmatrix} \epsilon_1 \\ \epsilon_2 \\ \gamma_{12} \end{bmatrix} = \begin{bmatrix} c^2 & s^2 & cs \\ s^2 & c^2 & -cs \\ -2cs & 2cs & c^2 - s^2 \end{bmatrix} \begin{bmatrix} \epsilon_x \\ \epsilon_y \\ \gamma_{xy} \end{bmatrix}, \tag{20}$$

where $c = \cos(\theta_i)$ and $s = \sin(\theta_i)$. Similar transformation in terms of stress is given as $\boldsymbol{\sigma} = \boldsymbol{T}_2(\boldsymbol{\eta})\boldsymbol{\sigma}_{loc}$,

$$\begin{bmatrix} \sigma_x \\ \sigma_y \\ \tau_{xy} \end{bmatrix} = \begin{bmatrix} c^2 & s^2 & -2cs \\ s^2 & c^2 & 2cs \\ cs & -cs & c^2 - s^2 \end{bmatrix} \begin{bmatrix} \sigma_1 \\ \sigma_2 \\ \tau_{12} \end{bmatrix}. \tag{21}$$

The homogenized constitutive relationship is given by:

$$\boldsymbol{\sigma}_{loc} = \boldsymbol{Q}(\boldsymbol{\xi})\boldsymbol{\epsilon}_{loc}, \tag{22}$$

where $\boldsymbol{Q}(\boldsymbol{\xi})$ is the reduced stiffness stiffness matrix

$$\boldsymbol{Q}(\boldsymbol{\xi}) = \begin{bmatrix} \frac{E_1}{1-v_{12}v_{21}} & \frac{v_{21}E_1}{1-v_{12}v_{21}} & 0 \\ \frac{v_{12}E_2}{1-v_{12}v_{21}} & \frac{E_2}{1-v_{12}v_{21}} & 0 \\ 0 & 0 & G_{12} \end{bmatrix}. \tag{23}$$

For the ith layer, the stress–strain relationship in global coordinates is given as:

$$\boldsymbol{\sigma} = \bar{\boldsymbol{Q}}_i(\boldsymbol{\xi}, \boldsymbol{\eta})\boldsymbol{\epsilon} = \boldsymbol{T}_2(\boldsymbol{\eta})\boldsymbol{Q}(\boldsymbol{\xi})\boldsymbol{T}_1(\boldsymbol{\eta})\boldsymbol{\epsilon}. \tag{24}$$

Integrating Eq. (24) in each layer through the thickness, we obtain the relationship between force/moment resultants and midplane strain/curvature as:

$$\begin{bmatrix} N \\ M \end{bmatrix} = \begin{bmatrix} A(\boldsymbol{\xi}, \boldsymbol{\eta}) & B(\boldsymbol{\xi}, \boldsymbol{\eta}) \\ B(\boldsymbol{\xi}, \boldsymbol{\eta}) & D(\boldsymbol{\xi}, \boldsymbol{\eta}) \end{bmatrix} \begin{bmatrix} \boldsymbol{\epsilon}^0 \\ \boldsymbol{\kappa} \end{bmatrix}, \tag{25}$$

where A, B and D are extensional, coupling, and bending stiffness matrices (Kaw 2005). Note the randomness in the stiffness matrices includes stochastic effective properties and stochastic fiber orientation, denoted by the random vectors $\boldsymbol{\xi}$ and $\boldsymbol{\eta}$, respectively.

Failure criteria may be applied with the stresses calculated from Eqs. (24) and (25). Some commonly used failure theories include the *maximum stress* failure theory

$$X_C < \sigma_1 < X_T, \ Y_C < \sigma_2 < Y_T, \ |\tau_{12}| < S \tag{26}$$

and the *Tsai–Wu* failure theory

$$F_{11}\sigma_1^2 + 2F_{12}\sigma_1\sigma_2 + F_{22}\sigma_2^2 + F_{66}\tau_{12}^2 + F_1\sigma_1 + F_2\sigma_2 < 1$$

$$F_{11} = \frac{1}{X_T X_C}, \ F_{22} = \frac{1}{Y_T Y_C}, \ F_{66} = \frac{1}{S^2}$$

$$F_1 = \frac{1}{X_T} - \frac{1}{X_C}, \ F_2 = \frac{1}{Y_T} - \frac{1}{Y_C}, \ F_{12} = -\frac{1}{2}\sqrt{F_{11}F_{22}},$$

$$(27)$$

where X_C and X_T are longitudinal compressive and tensile strength, Y_C and Y_T are transverse compressive and tensile strength, S is shear strength in the 1–2 plane. As the laminate is composed of multiple layers, the failure process is progressive and involves stress redistribution. Although the failure mechanisms are generally complex, a conservative approach of ply discounts of failed plies are often used in design from first-ply failure (FPF) to ultimate failure (UF). The FPF strength is the load at which the initiation of failure in the first ply, determined by the failure criterion. In the following stress analysis, the stiffness matrix of a partially failed layer is partially discounted as:

$$\boldsymbol{Q}(\boldsymbol{\xi}) = \begin{bmatrix} \frac{E_1}{1-v_{12}v_{21}} & 0 & 0 \\ 0 & 0 & 0 \\ 0 & 0 & 0 \end{bmatrix}, \qquad (28)$$

if fiber direction stress is below the failure strengths in the fiber direction, i.e., $X_C < \sigma_1 < X_T$. If fiber failure has occurred, full degradation is adopted, i.e., $\boldsymbol{Q} = 0$. The process of ply discounting continues as successive plies fail, until the last ply has failed, whereupon it is deemed to have reached its ultimate failure (UF) load.

3 Numerical implementation

The section describes the implementation of stochastic homogenization and failure analyses. Traditionally, it is difficult to implement spectral-based finite element method (SSFE) in a commercial FE package because its formulation is usually developed at the global stiffness matrix (Stefanou 2009). To overcome this difficulty, SSFE at element stiffness level has been formulated and implemented in UEL (user-defined elements) in ABAQUS®. From Eq. (16), the element stiffness, force matrices and solution variables can be written as:

$$\boldsymbol{k}^e = \begin{bmatrix} \boldsymbol{k}_{0,0}^e & \cdots & \boldsymbol{k}_{0,P_\chi-1}^e \\ \vdots & \ddots & \vdots \\ \boldsymbol{k}_{P_\chi-1,0}^e & \cdots & \boldsymbol{k}_{P_\chi-1,P_\chi-1}^e \end{bmatrix}, \boldsymbol{f}^e = \begin{bmatrix} \boldsymbol{f}_0^e \\ \vdots \\ \boldsymbol{f}_{P_\chi-1}^e \end{bmatrix}, \boldsymbol{X}^e = \begin{bmatrix} \boldsymbol{X}_0^e \\ \vdots \\ \boldsymbol{X}_{P_\chi-1}^e \end{bmatrix}.$$

$$(29)$$

The size of sub-matrices $\boldsymbol{k}_{ij}^e$ is equivalent to that of standard solid element, 8×8. Thus, the design of this new stochastic element requires more degrees of freedom, which is achieved by defining a superelement (called 'stochastic element' here) containing extra sets of nodes (8 nodes per set). The number of node sets is P_χ, which depends on the truncated terms in polynomial chaos expansion. Since the force matrix in Eq. (16) contains six column vectors, a linear perturbation step is adopted for the solution and six load cases in total are applied.

As shown in Fig. 4, a numerical model of single-fiber representative volume element with periodic boundary conditions is first created. Then the input file is modified for the purpose of spectral stochastic analysis and a UEL file is generated with a MATLAB® program. With the solution of Eq. (16), an explicit formulation of stochastic homogenized stiffness matrix is derived based on Eqs. (17) and (18). The probabilistic distribution of the effective properties can be reproduced through post-processing and sampling generation by Monte Carlo simulation (MCS). The up-scaled stochastic effective properties and other stochastic parameters are then provided as the input for the stochastic failure analysis. Sensitivity analysis could be performed by calculating the correlation of the input parameters with the output, which is a by-product of the stochastic analysis.

4 Results and discussion

In this section, a quasi-isotropic AS4/3501-6 laminate with lay-up of $[90^\circ/\pm 45^\circ/0^\circ]_s$ has been analyzed with uncertainties at both micro- and meso-scales. Based on the aforementioned methods, the probabilistic characteristics of effective properties of the lamina and strength values of the laminate are calculated.

4.1 Stochastic effective properties

Effective elastic properties of AS4/3501-6 composites were firstly estimated based on the constituent material properties. The fiber is transversely orthotropic and the matrix is isotropic, elastic properties of which are given as follows (average values): $E_1^f = 225\,\text{GPa}$, $E_2^f = 15\,\text{GPa}$, $G_{12}^f = 15\,\text{GPa}$, $v_{12}^f = 0.2$, $v_{23}^f = 0.07$; $E^m = 4.2\,\text{GPa}$, $v^m = 0.34$ (Soden et al. 1998; Zhou et al. (2016c)). The uncertainties in micro-scale properties are introduced uniformly in the stiffness matrices of fiber and matrix as:

$$\boldsymbol{D}(\boldsymbol{\xi}) = \boldsymbol{D}_0 + \boldsymbol{D}_1\xi_1 + \boldsymbol{D}_2\xi_2 = \begin{cases} \boldsymbol{D}^f + C_v\boldsymbol{D}^f\xi_1 & \text{fiber} \\ \boldsymbol{D}^m + C_v\boldsymbol{D}^m\xi_2 & \text{matrix,} \end{cases}$$

$$(30)$$

Fig. 4 Flow chart of stochastic two-scale analysis framework
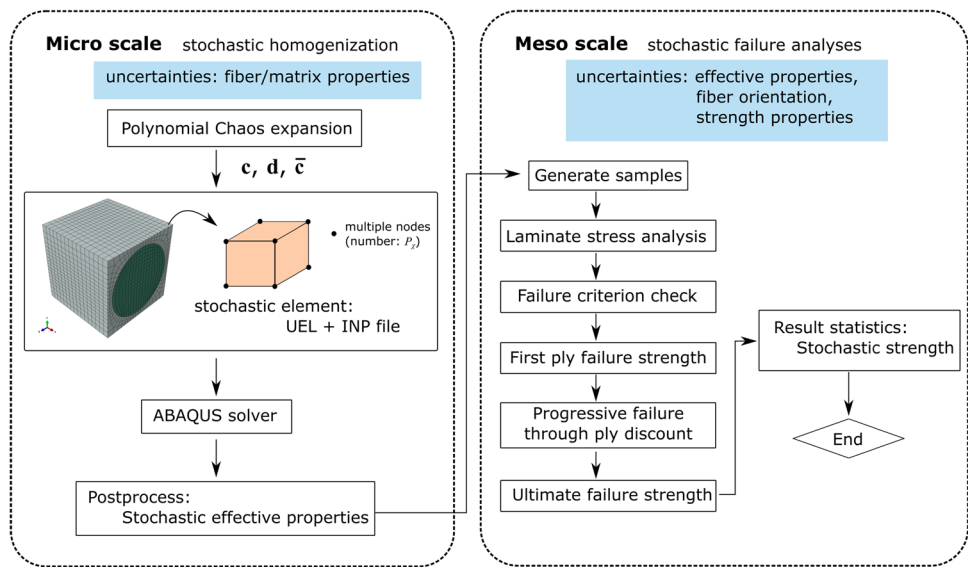
**Table 1** Polynomial chaos from order 1 to 3 ($\Psi_0 = 1$)

p	j	$\Psi_j(\xi_1, \xi_2)$
1	1–2	ξ_1, ξ_2
2	3–5	$\xi_1^2 - 1, \xi_1\xi_2, \xi_2^2 - 1$
3	6–9	$\xi_1^3 - 3\xi_1, \xi_2(\xi_1^2 - 1), \xi_1(\xi_2^2 - 1), \xi_2^3 - 3\xi_2$

where C_v is the coefficient of variation (COV) and ξ_1, ξ_2 are two independent random variables of standard normal distribution. Two cases were studied with small variation ($C_v = 0.1$) and large variation ($C_v = 0.2$), respectively. The truncated order in the PC expansion is tested from $p = 1$ to $p = 3$. Although higher accuracy is achieved with more terms, it also increases computational burden. The polynomial chaos corresponding to each order is given in Table 1. To verify the results by the method developed, Monte Carlo simulations were conducted with 10^4 samples. The convergence of the results (mean value and coefficient of variance of $D^h(1, 1)$ is shown in Fig. 5. The total CPU time for the MCS is 0.8×10^4 s (with a computer: four processors of Intel® Core™ i5-2400 CPU @ 3.10 GHz, 8 GB memory) while that for the spectral-based method with up to third-order terms is 6.74 s, which illustrates the efficiency of spectral stochastic homogenization method.

The coefficients in Eq. (13) are firstly calculated as the main solution variables as shown in Eq. (16). According to the properties of $\Psi_j(\boldsymbol{\xi})$, X_0 is the mean value of stochastic characteristic displacement $\boldsymbol{\chi}(\boldsymbol{\xi})$. An example of X_0 is given in Fig. 6, which shows the deformations of the RVE subjected to tension in each of the three directions (X, Y, Z) and shear in each of the three planes ($X - Y, Y - Z, X - Z$). Having obtained X_j, the coefficients in the expansion of stochastic homogenized stiffness matrix can be calculated through Eq.
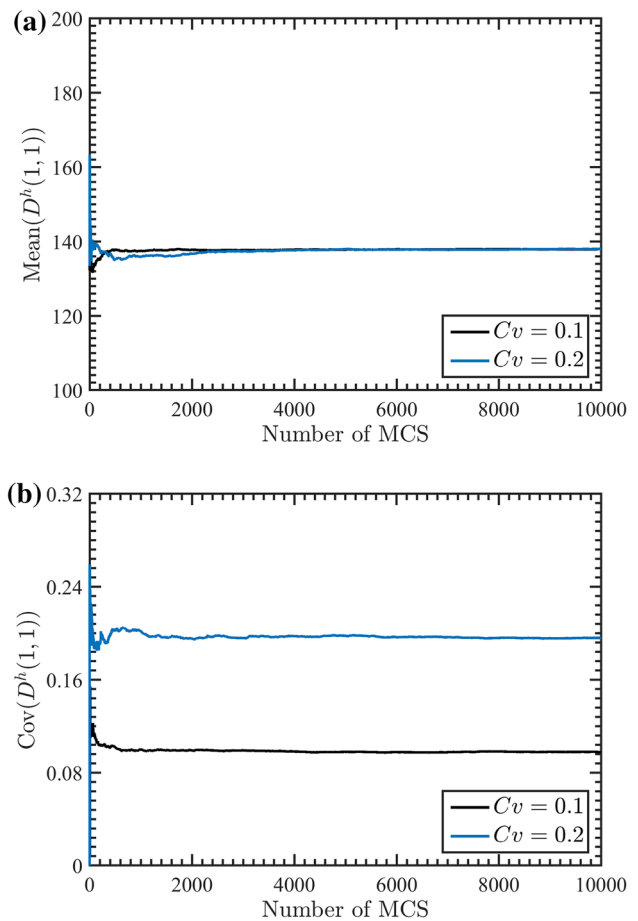
Fig. 5 Statistical convergence of **a** mean($D^h(1, 1)$), **b** Cov($D^h(1, 1)$) with MCS

(18). Through post-processing, the probability distribution of effective properties is plotted in Fig. 7 and compared with the results by MCS. It can be seen that high accuracy is
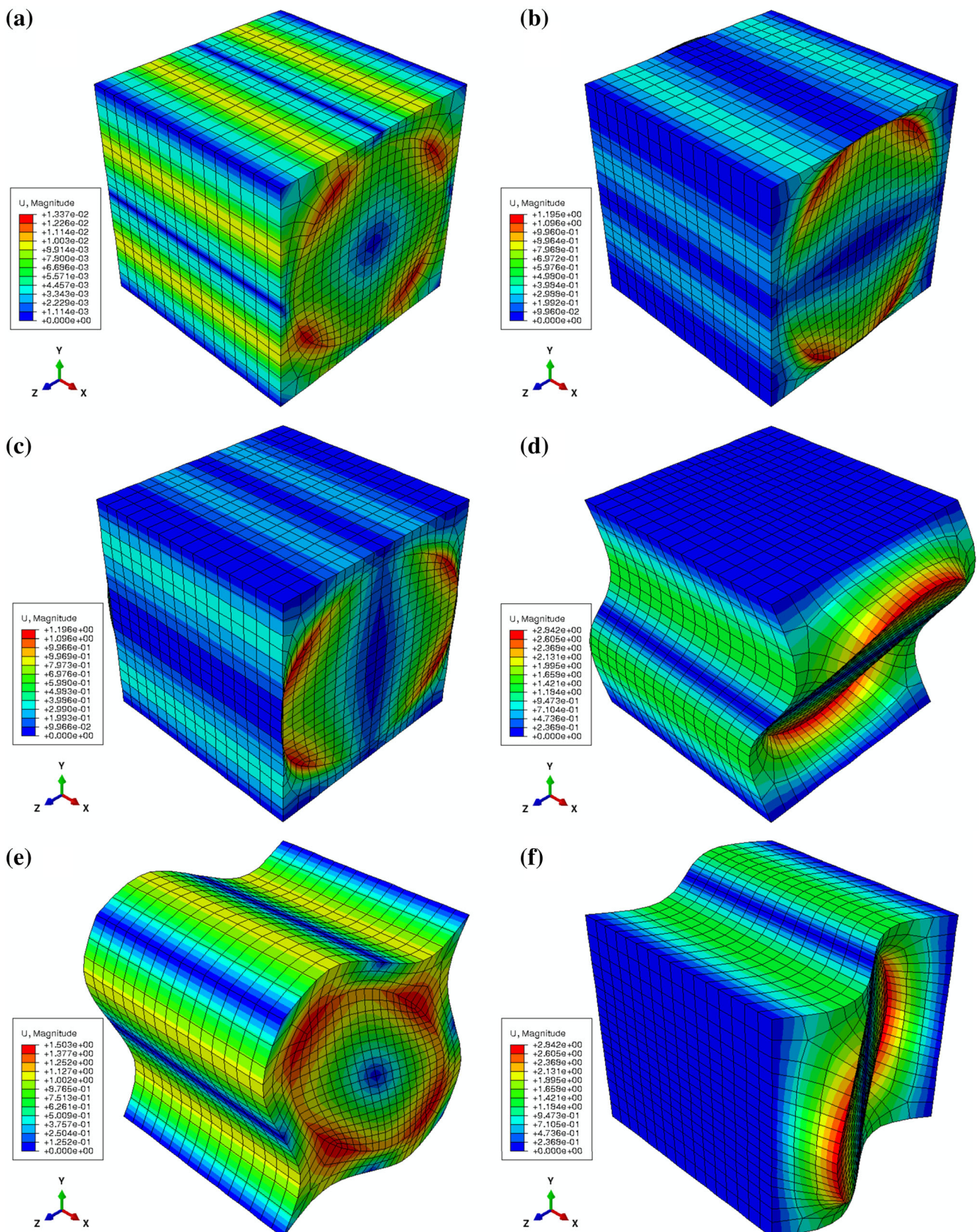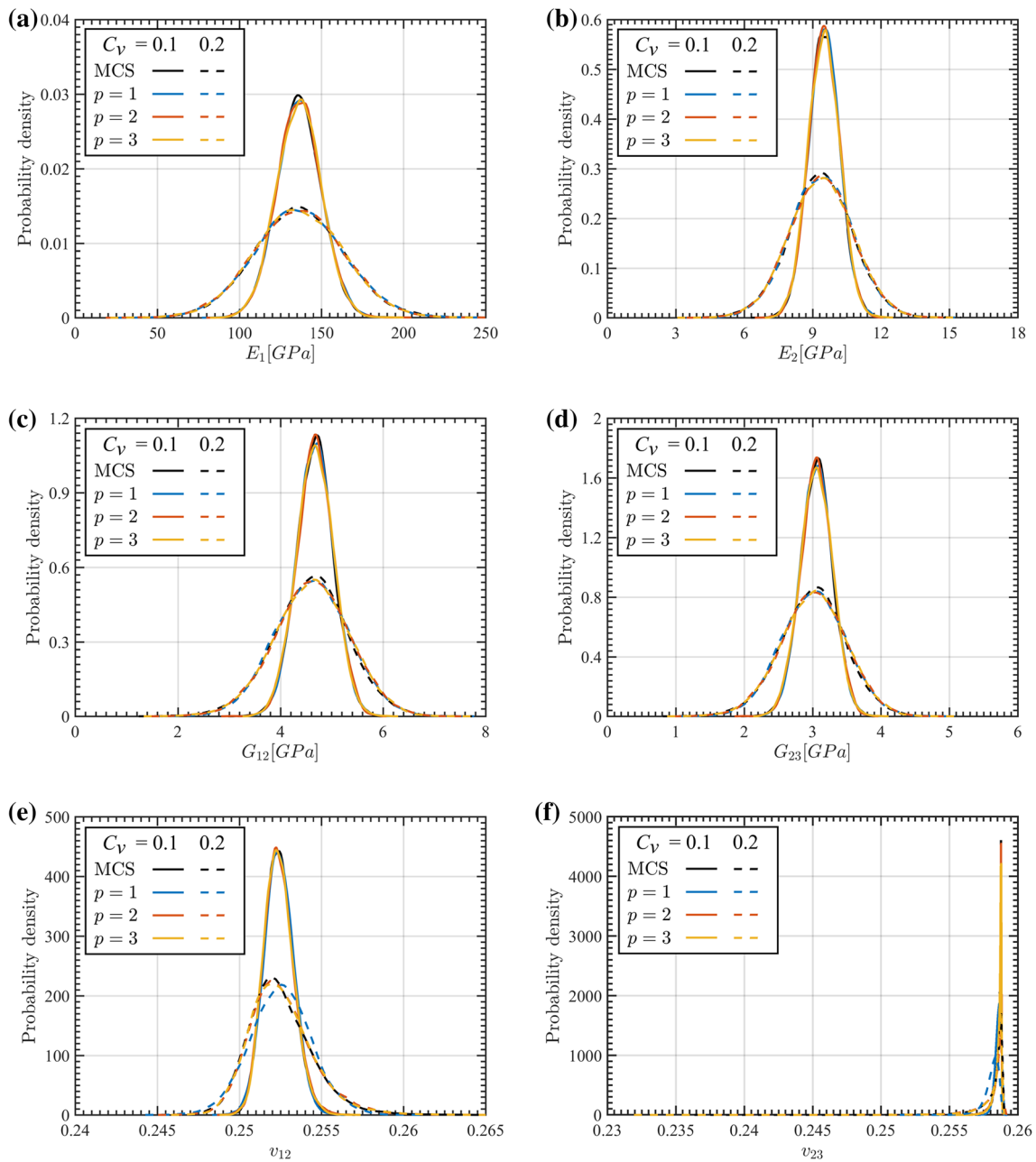
Fig. 6 The mean value of stochastic characteristic displacement for the case ($C_v = 0.2$) **a** 1st, **b** 2nd, **c** 3rd, **d** 4th, **e** 5th and **f** 6th column of X_0

Fig. 7 Probability distribution of stochastic effective properties by spectral-based method and MCS **a** E_1, **b** E_2, **c** G_{12}, **d** G_{23}, **e** v_{12}, **f** v_{23}

achieved with the new method for both cases ($C_v = 0.1$, 0.2) when second-order and third-order PC expansions are adopted. Only very small differences from the MCS results are found for the Poisson's ratios v_{12} and v_{23} with $p = 1$. The reason is that the first-order PC expansion in Table 1 is only capable of reproducing a linear combination of two Gaussian random variables. The statistics including mean value and standard deviation for the case with large variation are listed in Table 2 and comparisons are shown in Fig. 8. The coefficient of variation in E_1, E_2, G_{12} and G_{23} are all smaller than the input variation (0.2) and the variations in

v_{12} and v_{23} are extremely small, which illustrates that the randomness considered in stiffness matrix (due to moduli) hardly propagates to effective Poisson's ratio. Similarly, only the standard deviation in Poisson's ratio with $p = 1$ deviates from MCS results.

Besides the probability characteristic of individual effective properties, another feature that can be captured with stochastic analysis from micro-scale is the correlation among different properties. The correlation coefficients calculated by MCS and spectral-based method ($p = 2$) are given in Table 3. Strong correlation (defined as the absolute value of

Table 2 Statistics of effective properties by MCS ($C_v = 0.2$, moduli in GPa)

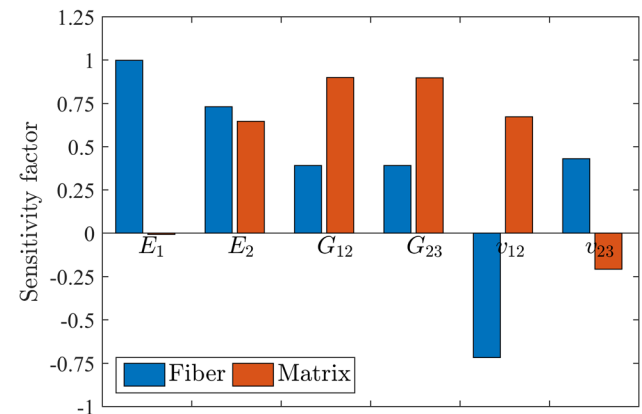| Properties	Mean	STD	COV
E_1	136.409	26.911	0.197
E_2	9.358	1.380	0.148
G_{12}	4.598	0.724	0.157
G_{23}	3.004	0.473	0.157
v_{12}	0.253	0.002	0.008
v_{23}	0.258	0.001	0.005

Table 3 Correlation of effective properties from results ($C_v = 0.2$) by MCS and spectral-based method with $p = 2$ (MCS-upper right triangular, spectral-lower left triangular)

Properties	E_1	E_2	G_{12}	G_{23}	v_{12}	v_{23}
E_1		0.736	0.407	0.408	−0.706	0.417
E_2	0.738		0.915	0.916	−0.109	0.344
G_{12}	0.404	0.914		1.000	0.287	0.157
G_{23}	0.405	0.914	1.000		0.286	0.159
v_{12}	−0.708	−0.112	0.291	0.290		−0.566
v_{23}	0.443	0.330	0.120	0.121	−0.608	
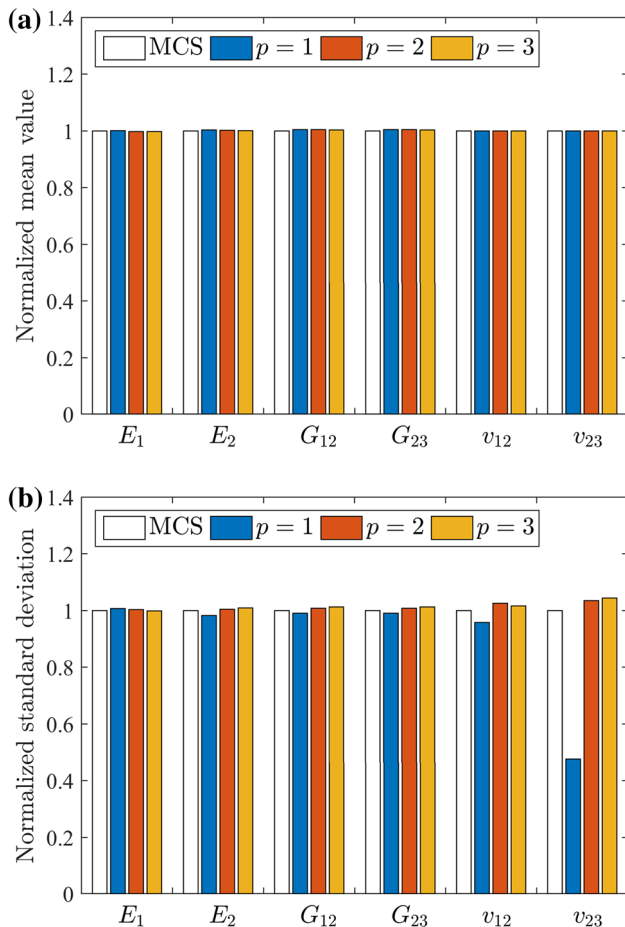
Fig. 8 Statistics of stochastic effective properties by spectral-based method and MCS ($C_v = 0.2$): **a** normalized mean value, **b** normalized standard deviation (results by MCS are adopted as baseline)

Fig. 9 Sensitivity factors of effective elastic properties with respect to variation of fiber and matrix properties

ties, sensitivity analysis can be conducted as a by-product of spectral homogenization, the results of which are plotted in Fig. 9. It can be observed that E_1 is sensitive to the variation of fiber properties while E_2 is correlated with both fiber and matrix constituents. The shear moduli are more influenced by randomness of matrix than that of fiber and v_{12} is more sensitive to constituent properties than v_{23}.

4.2 Stochastic strength predictions

The uncertainties of composites at micro-scale are propagated to meso-scale through stochastic homogenization, which results in the randomness in effective elastic properties. Since the elastic properties can affect the stress analysis of composite structures, these uncertainties are included in the stochastic strength calculation. For the sake of clarity, only the case with large variation ($C_v = 0.2$) analyzed in the previous section is studied here. Furthermore, additional uncertainties considered at meso-scale include ply strength properties and ply misalignment. The statistical properties are listed in Table 4, where strength parameters are treated as log-normal variables and misalignment angle is assumed normally distributed. The total thickness of the laminate with lay-up of $[90^o / \pm 45^o / 0^o]_s$ is $h = 1.1$ mm and each ply is

correlation coefficients larger than 0.5) can be found in pairs E_1/E_2, E_1/v_{12}, E_2/G_{12}, E_2/G_{23}, G_{12}/G_{23} and v_{12}/v_{23}. This information is usually absent in the stochastic analysis directly based on meso-scale, where the effective properties are assumed independent random variables (Zhou et al. 2016c). It should also be noted the correlation coefficients depend on the input random variables considered in the constituent properties. To evaluate the effect of variation of input parameters (ξ_1, ξ_2) on the stochastic effective elastic proper-

Table 4 Statistical properties of random variables at meso-scale (Zhou et al. 2016c; Chamis 2004)

	Random variable	Mean value (μ)	Standard deviation (σ)	Distribution
Strength	X_T	1969 MPa	0.1μ	Log-normal
	X_C	1480 MPa	0.12μ	Log-normal
	Y_T	48 MPa	0.06μ	Log-normal
	Y_C	200 MPa	0.08μ	Log-normal
	S	79 MPa	0.11μ	Log-normal
Ply misalignment	$\hat{\theta}$	0º	0.9º	Normal
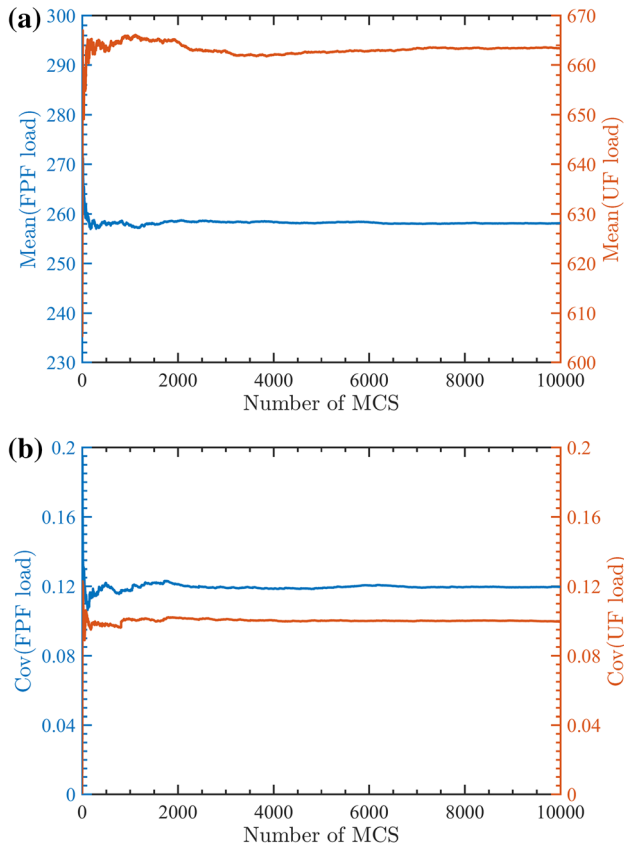
Fig. 10 Statistical convergence of **a** mean value, **b** coefficient of variation of FPF load and UF load (uniaxial tension, N_x/h)

Fig. 11 Probability distribution of FPF load and UF load of the laminate subject to **a** uniaxial loading, **b** biaxial loading ($N_x = 2N_y$) based on maximum stress and Tsai–Wu failure theory

of equal thickness. Two loading conditions are considered: one for uniaxial tension ($N_x > 0$) and the other for biaxial tension ($N_x = 2N_y > 0$). The first-ply failure (FPF) and ultimate failure (UF) loads are calculated with 10^4 samples (MCS). The statistical convergence of the mean and COV for the uniaxial tension case is illustrated in Fig. 10.

As shown by the distribution of the FPF load and UF load in Fig. 11, it can be observed that the scatter of UF load is larger than that of FPF load since the FPF load only depends on the strength of the weakest ply and progressive failure of all the plies influences the final failure. In addition, the Tsai–Wu criterion is more conservative in evaluating the UF load than maximum stress criterion but the difference in prediction

of FPF load is small. With the stochastic strength and given load variation, reliability factor of the composite plates can be evaluated for a limit state design. Furthermore, sensitivity analysis is implemented for understanding the effect of elastic properties (E_1, E_2, G_{12} and v_{12}), strength properties (X_t, X_c, Y_t, Y_c and S) and ply angles (θ_i, $i = 1, 2, \ldots, 8$) on the failure load. The results for two loading cases based on two criteria are given in Fig. 12. The FPF load is strongly correlated with E_1 and v_{12} among elastic properties and Y_t, which indicates transverse matrix crack occurs at first-ply failure.

Fig. 12 Sensitivity factor of FPF and UF load with respect to variations in inputs **a** unaxial loading, maximum stress criterion; **b** biaxial loading, maximum stress criterion; **c** unaxial loading, Tsai–Wu criterion; **d** biaxial loading, Tsai–Wu criterion
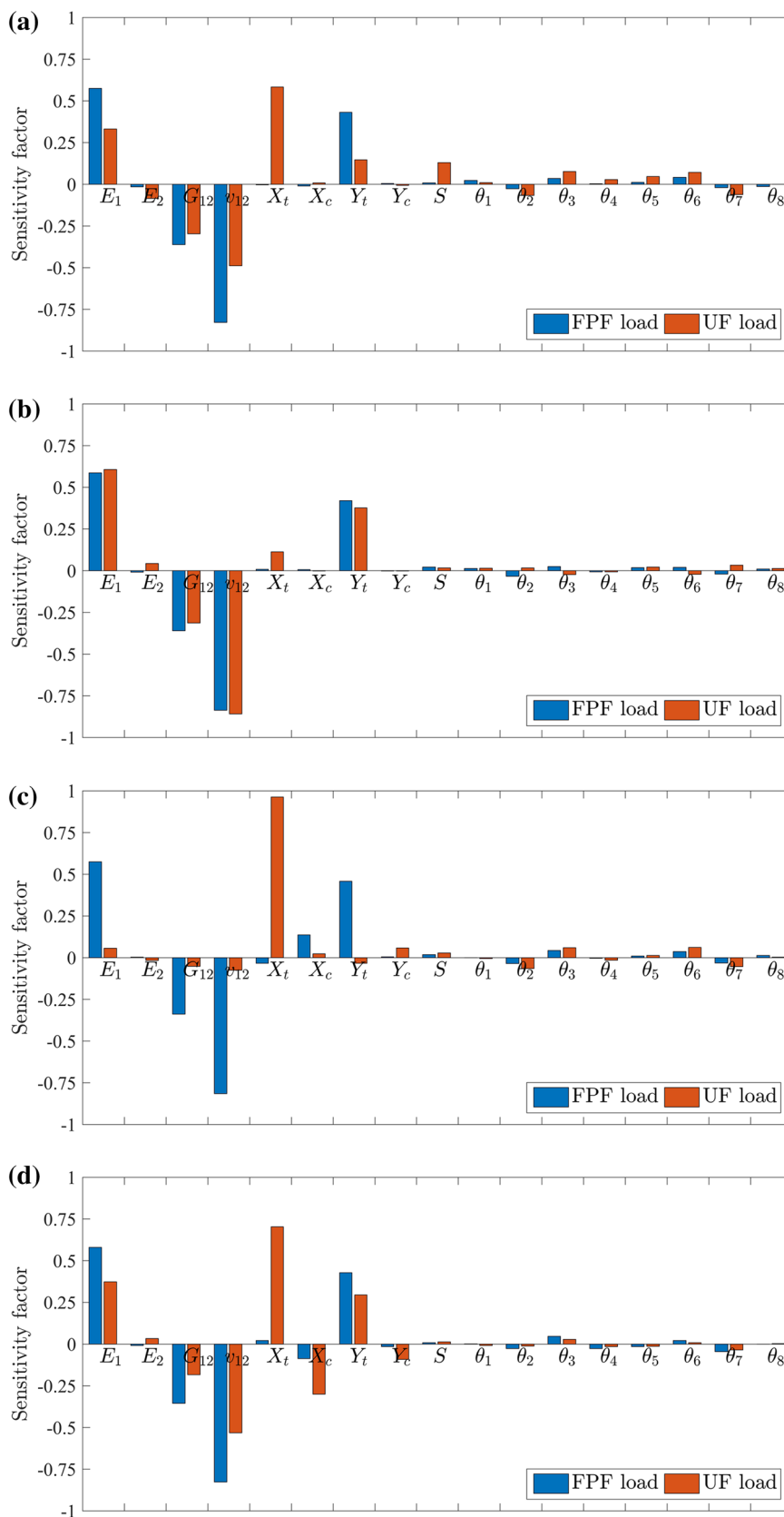
As for the ultimate failure, longitudinal tensile strength X_t plays an important role. Moreover, the effect of ply misalignment on failure load is not significant in the current study involving tensile loading, which indicates this type of geometric uncertainties can be ignored in future development of non-sampling-based stochastic methods at meso-scale. However, fiber misalignment and waviness may affect the compressive failure strength (Liu et al. 2004), but a more sophisticated model should be established.

An important feature of stochastic analysis from microscale is the correlation among effective elastic properties. To study the effect of the correlation on stochastic failure load, further analysis was conducted with uncorrelated E_1, E_2, G_{12} and v_{12}, which are generated by random sampling from previous results with the same probability distribution as shown in Fig. 7. The predicted results and previous ones are compared in Fig. 13 based on Tsai–Wu criterion. It can be observed that the probability distribution of the FPF load without considering the correlation becomes flatter than the results considering correlation while the predicted UF load distribution is very close. This observation agrees well with the sensitivity results in Fig. 12c that the UF load is not sensitive to the elastic properties. But for biaxial cases, the FPF load and UF load are both affected and the scatter of both becomes larger. The results illustrate the relevance of a proper characterization of the correlation information of material properties at ply level, which is usually absent in a meso-scale stochastic analysis.

5 Conclusion

In this paper, a spectral-based stochastic multi-scale method is proposed for computational structural analysis of composites with multi-uncertainties. Classical asymptotic homogenization method is employed to connect material properties at micro-scale and meso-scale. Uncertainty propagation between these two scales are achieved by combing asymptotic homogenization with the spectral stochastic finite element method. With two random variables standing for uncertainties in fiber and matrix taken into account, the probability structure of effective elastic properties is fully predicted with polynomial chaos expansion. The statistical results including probability distribution, statistical moments and correlation are compared with converged results by Monte Carlo simulations, which shows good agreements. By incorporating stochastic effective properties and other uncertainties at meso-scale, stochastic strength analysis of a quasi-isotropic composite laminate has been conducted with analytical approach and Monte Carlo simulations. Probability distribution of first-ply failure and ultimate failure load values are predicted, which can provide a basis for reliability analysis of composite structures. Furthermore, sensitivity
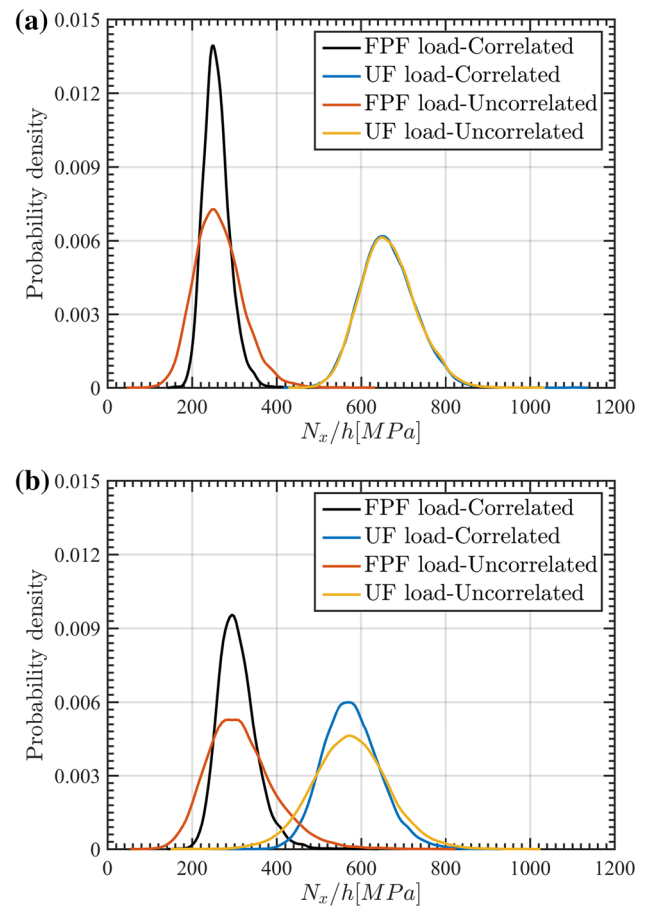
Fig. 13 Probability distribution of FPF load and UF load of the laminate subject to **a** uniaxial loading, **b** biaxial loading ($N_x = 2N_y$) based on Tsai–Wu failure theory and correlated and uncorrelated effective elastic properties

analysis shows that parameters such as E_1, v_{12}, X_t and Y_t are critical while the parameters θ_i hardly affect stochastic outputs in current analysis of tensile strength, which indicates the dimension of this stochastic problem can be reduced for the uniaxial and biaxial tensile load cases studied here. Besides, a further analysis with uncorrelated effective properties shows larger scatter in the stochastic failure load prediction. It implies that a meso-scopic stochastic analysis cannot achieve reasonable prediction unless the correlations among material properties are quantified in advance.

In conclusion, this work proposes a computational framework combining different mechanics models and probability methods and illustrates stochastic multi-scale analysis of composite structures through numerical examples. As regards the uncertainty propagation from micro-scale to meso-scale, the spectral stochastic finite element method is efficient, however, the application of which is usually limited in engineering due to its intrusive formulation. To this end, a specific type of element with variable nodes is developed and implemented in a commercial FE package.

Although only Gaussian random distribution is considered in this work, other types of distribution can be included in this framework by employing generalized polynomial chaos (Xiu 2010). Future development of this framework with nonlinear mechanics may consider the collocation method (Panayirci and Schuëller 2011), which is promising in stochastic analysis of complicated problems. Finally, to build an integral framework of stochastic analysis of composite structures, frequency statistics of large amount of test data or stochastic inverse analysis based on limited available experimental data is necessary for the quantification of uncertainties in the input of current analysis.

References

Andersons J, Joffe R, Spārniņš E (2008) Statistical model of the transverse ply cracking in cross-ply laminates by strength and fracture toughness based failure criteria. Eng Fract Mech 75(9):2651–2665

Arregui-Mena JD, Margetts L, Mummery PM (2016) Practical application of the stochastic finite element method. Arch Comput Methods Eng 23(1):171–190

Balokas G, Czichon S, Rolfes R (2017) Neural network assisted multiscale analysis for the elastic properties prediction of 3d braided composites under uncertainty. Compos Struct 183:550–562

Chakraborty S, Mandal B, Chowdhury R, Chakrabarti A (2016) Stochastic free vibration analysis of laminated composite plates using polynomial correlated function expansion. Compos Struct 135:236–249

Chamis CC (2004) Probabilistic simulation of multi-scale composite behavior. Theor Appl Fract Mech 41(1):51–61

Charmpis DC, Schuëller GI, Pellissetti MF (2007) The need for linking micromechanics of materials with stochastic finite elements: a challenge for materials science. Comput Mater Sci 41(1):27–37

Chen X, Qiu ZP (2018) A novel uncertainty analysis method for composite structures with mixed uncertainties including random and interval variables. Compos Struct 184:400–410

Chen NZ, Soares CG (2008) Spectral stochastic finite element analysis for laminated composite plates. Comput Methods Appl Mech Eng 197(51):4830–4839

Chen N, Yu DJ, Xia BZ, Liu J, Ma ZD (2017) Interval and subinterval homogenization-based method for determining the effective elastic properties of periodic microstructure with interval parameters. Int J Solids Struct 106:174–182

Chiachio M, Chiachio J, Rus G (2012) Reliability in composites—a selective review and survey of current development. Compos Part B Eng 43(3):902–913

Chung DB, Gutiérrez MA, de Borst R (2005) Object-oriented stochastic finite element analysis of fibre metal laminates. Comput Methods Appl Mech Eng 194(12):1427–1446

Cui XY, Hu XB, Zeng Y (2017) A copula-based perturbation stochastic method for fiber-reinforced composite structures with correlations. Comput Methods Appl Mech Eng 322:351–372

Dey S, Mukhopadhyay T, Adhikari S (2015) Stochastic free vibration analyses of composite shallow doubly curved shells—a Kriging model approach. Compos B Eng 70:99–112

Dey S, Mukhopadhyay T, Adhikari S (2017) Metamodel based high-fidelity stochastic analysis of composite laminates: a concise review with critical comparative assessment. Compos Struct 171:227–250

Ghanem RG, Spanos PD (2003) Stochastic finite elements: a spectral approach. Courier Corporation, North Chelmsford

Jeong HK, Shenoi RA (2000) Probabilistic strength analysis of rectangular FRP plates using Monte Carlo simulation. Comput Struct 76(1):219–235

Kamiński M, Kleiber M (2000) Perturbation based stochastic finite element method for homogenization of two-phase elastic composites. Comput Struct 78(6):811–826

Karsh PK, Mukhopadhyay T, Dey S (2018) Spatial vulnerability analysis for the first ply failure strength of composite laminates including effect of delamination. Compos Struct 184:554–567

Kaw Autar K (2005) Mechanics of composite materials. CRC Press, Boca Raton

Kepple J, Herath MT, Pearce G, Prusty BG, Thomson R, Degenhardt R (2015) Stochastic analysis of imperfection sensitive unstiffened composite cylinders using realistic imperfection models. Compos Struct 126:159–173

Lal A, Singh BN, Kumar R (2009) Effects of random system properties on the thermal buckling analysis of laminated composite plates. Comput Struct 87(17):1119–1128

Lal A, Singh BN, Kale S (2011) Stochastic post buckling analysis of laminated composite cylindrical shell panel subjected to hygrothermomechanical loading. Compos Struct 93(4):1187–1200

Lekou DJ, Philippidis TP (2008) Mechanical property variability in FRP laminates and its effect on failure prediction. Compos B Eng 39(7–8):1247–1256

Li JQ, Tian XP, Han ZJ, Narita Y (2016) Stochastic thermal buckling analysis of laminated plates using perturbation technique. Compos Struct 139:1–12

Liu D, Fleck NA, Sutcliffe MPF (2004) Compressive strength of fibre composites with random fibre waviness. J Mech Phys Solids 52(7):1481–1505

Lopez RH, Miguel LFF, Belo IM, Cursi JES (2014) Advantages of employing a full characterization method over form in the reliability analysis of laminated composite plates. Compos Struct 107:635–642

Lorca JL, González C, Molina-Aldareguía JM, Segurado J, Seltzer R, Sket F, Rodríguez M, Sádaba S, Muñoz R, Canal LP (2011) Multiscale modeling of composite materials: a roadmap towards virtual testing. Adv Mater 23(44):5130–5147

Ma J, Temizer I, Wriggers P (2011) Random homogenization analysis in linear elasticity based on analytical bounds and estimates. Int J Solids Struct 48(2):280–291

Nakayasu H, Maekawa Z (1997) A comparative study of failure criteria in probabilistic fields and stochastic failure envelopes of composite materials. Reliab Eng Syst Saf 56(3):209–220

Ngah MF, Young A (2007) Application of the spectral stochastic finite element method for performance prediction of composite structures. Compos Struct 78(3):447–456

Noh HC, Park T (2011) Response variability of laminate composite plates due to spatially random material parameter. Comput Methods Appl Mech Eng 200(29):2397–2406

Onkar AK, Upadhyay CS, Yadav D (2007) Probabilistic failure of laminated composite plates using the stochastic finite element method. Compos Struct 77(1):79–91

Panayirci HM, Schuëller GI (2011) On the capabilities of the polynomial chaos expansion method within SFE analysis—an overview. Arch Comput Methods Eng 18(1):43–55

Perić D, de Souza Neto EA, Feijóo RA, Partovi M (2011) On micro-to-macro transitions for multi-scale analysis of non-linear heterogeneous materials: unified variational basis and finite element implementation. Int J Numer Meth Eng 87(1–5):149–170

Pimenta S (2017) A computationally-efficient hierarchical scaling law to predict damage accumulation in composite fibre-bundles. Compos Sci Technol 146:210–225

Pimenta S, Pinho ST (2013) Hierarchical scaling law for the strength of composite fibre bundles. J Mech Phys Solids 61(6):1337–1356

Sakata S, Ashida F, Kojima T, Zako M (2008) Three-dimensional stochastic analysis using a perturbation-based homogenization method for elastic properties of composite material considering microscopic uncertainty. Int J Solids Struct 45(3):894–907

Sánchez-Heres LF, Ringsberg JW, Johnson E (2014) Influence of mechanical and probabilistic models on the reliability estimates of fibre-reinforced cross-ply laminates. Struct Saf 51:35–46

Scarth C, Cooper JE, Weaver PM, Silva GHC (2014) Uncertainty quantification of aeroelastic stability of composite plate wings using lamination parameters. Compos Struct 116:84–93

Sepahvand K (2016) Spectral stochastic finite element vibration analysis of fiber-reinforced composites with random fiber orientation. Compos Struct 145:119–128

Shaw A, Sriramula S, Gosling PD, Chryssanthopoulos MK (2010) A critical reliability evaluation of fibre reinforced composite materials based on probabilistic micro and macro-mechanical analysis. Compos B Eng 41(6):446–453

Soden PD, Hinton MJ, Kaddour AS (1998) Lamina properties, lay-up configurations and loading conditions for a range of fibre-reinforced composite laminates. Compos Sci Technol 7(58):1011–1022

Sriramula S, Chryssanthopoulos MK (2009) Quantification of uncertainty modelling in stochastic analysis of frp composites. Compos A Appl Sci Manuf 40(11):1673–1684

Stefanou G (2009) The stochastic finite element method: past, present and future. Comput Methods Appl Mech Eng 198(9):1031–1051

St-Pierre L, Martorell NJ, Pinho ST (2017) Stress redistribution around clusters of broken fibres in a composite. Compos Struct 168:226–233

Swolfs Y, Verpoest I, Gorbatikh L (2016) A review of input data and modelling assumptions in longitudinal strength models for unidirectional fibre-reinforced composites. Compos Struct 150:153–172

Tay TE, Liu G, Tan VBC, Sun XS, Pham DC (2008) Progressive failure analysis of composites. J Compos Mater 42(18):1921–1966

Tootkaboni M, Graham-Brady L (2010) A multi-scale spectral stochastic method for homogenization of multi-phase periodic composites with random material properties. Int J Numer Meth Eng 83(1):59–90

Van Vinckenroy G, De Wilde WP (1995) The use of Monte Carlo techniques in statistical finite element methods for the determination of the structural behaviour of composite materials structural components. Compos Struct 32(1–4):247–253

Vijaya Kumar RL, Bhat MR (2015) Probabilistic stress variation studies on composite single lap joint using Monte Carlo simulation. Compos Struct 121:351–361

Vinogradov V, Hashin Z (2005) Probabilistic energy based model for prediction of transverse cracking in cross-ply laminates. Int J Solids Struct 42(2):365–392

Wu WF, Cheng HC, Kang CK (2000) Random field formulation of composite laminates. Compos Struct 49(1):87–93

Xiu DB (2010) Numerical methods for stochastic computations: a spectral method approach. Princeton University Press, Princeton

Zhao LB, Shan MJ, Liu FR, Zhang JY (2017) A probabilistic model for strength analysis of composite double-lap single-bolt joints. Compos Struct 161:419–427

Zhou XY, Gosling PD, Pearce CJ, Kaczmarczyk Ł, Ullah Z (2016) Perturbation-based stochastic multi-scale computational homogenization method for the determination of the effective properties of composite materials with random properties. Comput Methods Appl Mech Eng 300:84–105

Zhou XY, Gosling PD, Pearce CJ, Ullah Z, Kaczmarczyk Ł (2016) Perturbation-based stochastic multi-scale computational homogenization method for woven textile composites. Int J Solids Struct 80:368–380

Zhou XY, Gosling PD, Ullah Z, Kaczmarczyk Ł, Pearce CJ (2016) Exploiting the benefits of multi-scale analysis in reliability analysis for composite structures. Compos Struct 155:197–212

Zhou XY, Gosling PD, Ullah Z, Kaczmarczyk Ł, Pearce CJ (2017) Stochastic multi-scale finite element based reliability analysis for laminated composite structures. Appl Math Model 45:457–473